Interaction of neoclassical tearing modes with externally applied magnetic perturbations at ASDEX Upgrade

S. Fietz[1], I. Classen[2], M. Garcia-Muñoz[3], H. Zohm[1], A. Bergmann[1], M. Maraschek[1], W. Suttrop[1] and the ASDEX Upgrade Team

[1] *Max Planck Institute for Plasma Physics, EURATOM Association , Garching, Germany*
[2] *FOM Institute DIFFER-Dutch Institute for Fundamental Energy Research, Association EURATOM-FOM, Nieuwegein, The Netherlands*
[3] *Faculty of Physics, FAMN Dpt.,University of Seville, Seville, Spain*

1. Introduction

Externally applied magnetic perturbations (MPs) are of great interest for the operation of future fusion devices. They are used for active MHD control, especially for the mitigation of edge localised modes. Also the favourable stabilising effect of rotating MPs on resistive wall modes [1] and neoclassical tearing modes [2] has already been shown. However, especially static externally applied MPs can additionally act on the plasma stability in an unfavourable way.

Magnetic islands can be influenced by externally applied magnetic perturbation fields which are produced by currents flowing in external coils in two ways: The resonant components of the MP field can penetrate trough the plasma and provoke magnetic reconnection at a resonant surface which is accompanied with the generation of a magnetic island. This island can act as seed island for a neoclassical tearing mode. Static resonant magnetic perturbations can hence produce a locked mode which in most of the cases even leads to a disruption. Also previously existing rotating modes can interact with the resonant MP fields. They are slowed down and lock to the MP field. The non resonant component of the error field does not influence MHD modes directly but instead induces a global torque, the so called neoclassical toroidal viscous torque (NTV), and hence also influences the critical error field strength for the appearance of locked modes [3].

The ASDEX Upgrade tokamak has recently been equipped with a set of 16 in-vessel saddle coils. They are installed at the low field side in two rows above and below the mid plane. This set of coils, the so called B-coils, enables the generation of magnetic perturbations with a toroidal mode number of $n \leq 4$. This low n mode spectrum is perfectly suitable to study the influence of the MPs on the (m/n)=(3/2) and (2/1) NTMs (m the poloidal and n the toroidal mode number) which are the most common and confinement degrading NTMs in ADSDEX Upgrade.

In this paper experimental observation are compared to modelling results. To study the influence of MPs on NTMs the frequency and width evolution can be modelled solving the modified Rutherford equation and the equation of motion including the MPs as described in [4].

2. Theoretical background

The resonant component of the perturbation field leads to a discontinuity in the perturbed helical poloidal flux at the resonant surfaces which implies the existence of a helical current flowing at these surfaces [4]. This helical current interacts with a magnetic island in two ways: it modifies the island width evolution due to an influence on the island stability, which can be described by a modified Rutherford equation. This interaction takes place for the component of the current that is in phase with the magnetic island ($\cos(\Delta\phi)$). On the other hand the $\sin(\Delta\phi)$ component of the current causes a (j$\times$B)-torque which is acting on the island in order to adapt the frequency of the mode to the frequency of the perturbation field. These two effects can be included into the modified Rutherford equation (1) and the equation of motion (2) [4]:

$$0.82\frac{\tau_R}{r_{\rm res}^2}\frac{dW}{dt} = \Delta' + \Delta_{\rm BS} + \Delta_{\rm ext} \qquad \Delta_{\rm ext} == \frac{2m_{\rm pol}}{r_{\rm res}}\left(\frac{W_{\rm vac}}{W}\right)^2 \cos(\Delta\phi) \qquad (1)$$

$$I\frac{d\omega}{dt} = T_{\rm vs} + T_{\rm jxB} + T_{\rm rw} + T_{\rm NTV} \qquad T_{\rm jxB} = -4\pi^2\frac{mn}{\mu_0} C^2\, W_{\rm vac}^2\, W^2\, \sin(\Delta\phi) \qquad (2)$$

The parameter C is defined as $(r_{\rm res}B_{\rm tor}|q'|)/(16q^2R_0)$. The perturbation caused by the externally applied magnetic fields has been parametrised in eq. (1) and (2) using the vacuum field approximation. Superimposing the vacuum perturbation of the field coils with the unperturbed magnetic equilibrium field approximates the vacuum island width, which is proportional to $\sqrt{\Psi_{\rm vac}}$.

The NTV is generated by a non ambipolar radial flow of trapped particles Γ which arises from the breaking of the axis-symmetry of the magnetic field caused by the non-resonant components of the external perturbation and contributes to the plasma rotation damping. Calculations following [5], [6] and [7] show that at ASDEX Upgrade the influence of the NTV is negligible small. In consequence, the NTV induced torque is neglected in the following calculation and not included in the equation of motion.

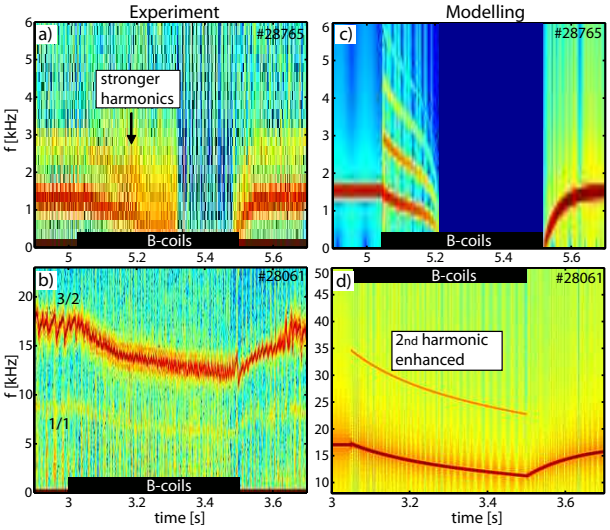

Figure 1: Experimental spectrograms of a pick-up coil signal for discharge #28765 a) and #28061 b). Panel c) and d) show the corresponding simulated spectrograms based on the modelling results.

Beside the resonant component of the MPs in the Rutherford equation, used for the modelling, approximations for the Δ' $(=-m/r_{\rm res})$ term and the destabilising contribution of the bootstrap current, which is proportional to $1/W$, are included. The equation of motion additionally contains a viscous torque and the torque induced by the resistive wall [8], which is mainly important for slowly rotating islands.

3. Experiment

In the following, two ASDEX Upgrade discharges are analysed in detail. In both discharges a clear impact of the MPs on NTMs is observed (figure 1 a) and b)). In discharge #28765, at low plasma rotation and medium $\beta_{\rm N} = 1.35$, a 2/1 NTM locks to the static MP field , whereas in discharge #28061, with a dedicated plasma shape, lower toroidal field, higher $\beta_{\rm N} = 2.1$ and substantial rotation, a 3/2 NTM is slowed down. Both islands spin up as soon as the B-coils are switched off (figure 1). The plasma rotation in both discharges decreases globally over the whole plasma radius during the B-coil phases. The rotation in the locked mode discharge decreases gradually and changes into counter-current direction for $\rho_{\rm pol} < 0.7$ during the locking phase, whereas at the mode position the toroidal plasma rotation approaches zero. In the braking case (#28061) the toroidal rotation profile is almost flat from the mode location towards the core which is consistent with the coupling of the n=2 component/harmonic of the 1/1 mode and the 3/2 NTM, which can be seen in figure 1 b). Based on equation (1) and (2) the influence of a resonant torque on a rotating island leads to a modulation of the mode amplitude and rotation frequency, and in consequence leads to a temporal modulation of the radial magnetic perturbation field induced by the mode.

This can be measured with pick-up coils at the edge of the plasma. This is particularly pronounced in the first discharge e.g. visible due to the enhancement of the higher harmonics in figure 1 a) and the distortion of the experimental pick-up coil signals (figure 2 a)). In the second discharge which is at higher plasma rotation, the effect of the B-coils is expected to be smaller. Consistent with this no big distortion of the magnetic signal can be found.

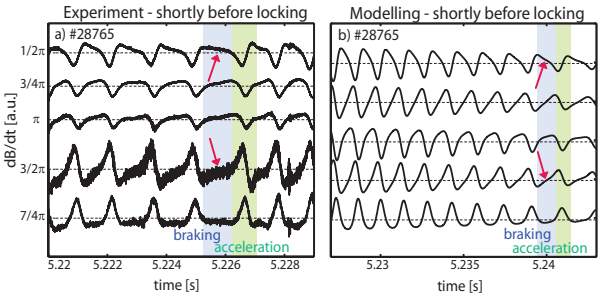

Figure 2: Pick-up coil signal at different toroidal positions discharge #28765. In a) the experimental signals and in b) the modelled signals shortly before mode locking are shown.

4. Modelling

The interaction of a saturated magnetic island with the externally applied MPs can be calculated, solving the coupled equation system for the mode amplitude eq. (1) and phase eq. (2).

Since the theory applied is developed for cylindrical plasmas, the quantities taken from the experiment with toroidal geometry have to be adjusted. This is done by using a flux surface averaged W_{vac} for the real ASDEX Upgrade geometry. The viscous torque is adjusted in the way that after switching off the B-coils the mode spins up to its natural frequency ω_0 in the time observed in the experiment. Mode coupling is not included. The modelling results for the frequency and the island width evolution are shown in figure 3 for both discharges. To match the experimental frequency evolution in both cases the parameter W_{vac} in equation (1) and (2) had to be increased by a factor c_{vac} of 2.2 for discharge #28765 and 4 for #28061 ($W_{\mathrm{vac,eff}} = c_{\mathrm{vac}} W_{\mathrm{vac}}$). This however not only increases the effect of the perturbation field on the island frequency but also on the island width evolution, which would lead to a stabilisation of the mode before locking in #28765. To prevent this, for the modelling of #28765, despite the fact that different perturbation field strength effecting the island width and frequency are not physical, the Δ_{ext} in equation (1) was reduced by a factor of 0.65, which in the end leads to an effective $W_{\mathrm{vac,eff}}$ in eq. (1) of $1.45 \cdot W_{\mathrm{vac}}$. Despite these adjustments the mode locks earlier than in experiment. The frequency evolution of the braking case (#28061) is well reproduced. Also in this discharge the stabilising effect of the MPs is overestimated compared to the experiment. For discharge #28765, also in the modelling, a strong modulation of the island width and frequency is found, as can be seen in the distortion of the simulated pick-up coil signal (figure 2 b)) and the strong enhancement of the higher harmonics in figure 1 c). In the modelling, like in experiment, these effects are less distinct for #28061, the braking case, since the enhancement of higher harmonics in 1 d) is less pronounced.

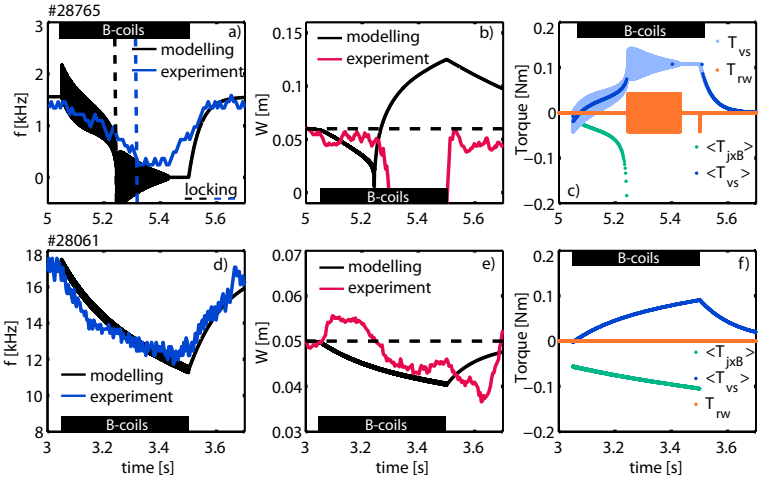

Figure 3: Calculated mode frequency a)+d) and island width b)+e) compared to the experimental quantities. c)+f) Time evolution of the acting torques (<> indicates an average over 2π). The dashed lines indicate the locking time point in experiment and modelling for discharge #28765.

Additionally, for discharge #28061, the evolution of the whole rotation profile is calculated

(fig. 4 b)), solving eq. (2) accounting for the radial dependence of the torques and a constant diffusion coefficient D_Φ of around $0.45\,m^2/s$. This diffusion coefficient D_Φ is determined by balancing the NBI input torque against the viscous torque to achieve the unperturbed rotation profile, shown in figure 4 a) in blue.

To match the flat rotation profile, which is present shortly before switching on the B-coils (fig. 4 green), mode coupling of the n=2 component of the 1/1 mode and the 3/2 NTM is qualitatively included, by adding equal but opposite torques at the q=1 and 3/2 surface (and in between). Additionally the toroidal rotation at the separatrix is a free parameter to adjust the profiles. To reproduce the decrease of the rotation profile of around 5 kHz observed in experiment due to the B-coils (green to red profile), a local (j×B)-torque of 0.15 Nm at the q=3/2 surface is needed, which is almost the same than the 0.1 Nm calculated before (see figure 3). Important here is that exactly the same rotation profile can be achieved when conserving the total (j×B)-torque but exerting fractions of it at different radial positions, hence at other rational surfaces.

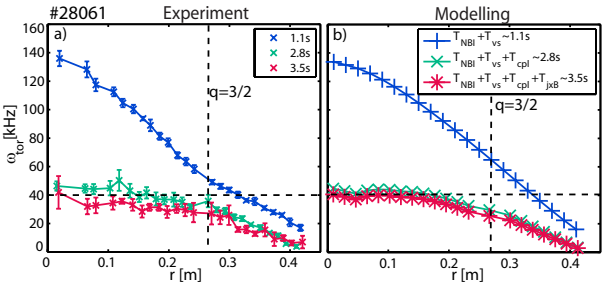

Figure 4: In a) the experimental rotation profiles are shown at the beginning of the discharge (1.1s) where no modes are present, before switching on the B-coils (2.8s) and at the end of the B-coil phase (3.5). In b) the modelled rotation profiles are shown, where the colour coding corresponds to a)

5. Conclusion

The mode braking as well as the modulation of the island width, corresponding to the influence of the resonant MP field components, are visible in the experiment and can be reproduced by the modelling. In both modelling cases the influence of the perturbation on the mode had to be increased, compared to the calculated vacuum values, to match the experimental frequency evolution whereas in consequence the stabilising effect on the mode is overestimated. Since such a large "field amplification" is, if at all, expected at the edge [9] and NTV is negligibly small for the analysed discharges, one possibility to explain the need of these MP field amplification, is that the all resonant torques at different resonant surfaces have to be taken into account. The sum of these different small resonant torques could in the end sum up to a total torque which has the same effect on the toroidal rotation than one big local one. This additionally leads to a smaller effective perturbation at the resonant surface and hence a smaller effect on the island width, comparable to the experiment. This is supported by the fact that also in the vacuum calculations islands at various rational surfaces are visible and that the error field direction, determined from the modelling, does not agree with the position of the $2/1$ vacuum island for #28765. Concluding the non resonant components of the perturbation field seems to be negligible at ASDEX Upgrade but the resonant torques at different resonant surfaces act together as a global resonant torque and are in combination responsible for the rotation damping.

References

[1] E. J. Strait et al, Physics of Plasmas **11**, 5 (2004)
[2] Qiming Hu et al, Nuclear Fusion **52**, 8 (2012)
[3] A. J Cole, Phys. Rev. Lett. **99**, (2007)
[4] R. Fitzpatrick, Nuclear Fusion **33**, 7 (1993)
[5] A.J. Cole et al, UW CPTC Report 08-8, University of Wisconsin, Madison, (2009)
[6] K. C. Shaing, Physics of Plasmas **10**, 5 (2003)
[7] J.D. Callen et al, Nuclear Fusion **49**, 8 (2009)
[8] H. Zohm et al, Europhysics Letters, **11**, 8 (1990)
[9] M. Garcia-Munoz et al, PPCF in preparation / 40^{th} EPS Finland 2013 (I5.114)